

## First Observation of the Unbound Nucleus $^{15}\text{Ne}$

F. Wamers,<sup>1,2,3,4</sup> J. Marganec,<sup>1,2,3</sup> F. Aksouh,<sup>2</sup> Yu. Aksyutina,<sup>2</sup> H. Álvarez-Pol,<sup>5</sup> T. Aumann,<sup>1,2</sup> S. Beceiro-Novo,<sup>5</sup> K. Boretzky,<sup>2</sup> M. J. G. Borge,<sup>6</sup> M. Chartier,<sup>7</sup> A. Chatillon,<sup>2</sup> L. V. Chulkov,<sup>2,8</sup> D. Cortina-Gil,<sup>5</sup> H. Emling,<sup>2</sup> O. Ershova,<sup>2,9</sup> L. M. Fraile,<sup>10</sup> H. O. U. Fynbo,<sup>11</sup> D. Galaviz,<sup>6</sup> H. Geissel,<sup>2</sup> M. Heil,<sup>2</sup> D. H. H. Hoffmann,<sup>1</sup> H. T. Johansson,<sup>12</sup> B. Jonson,<sup>12</sup> C. Karagiannis,<sup>2</sup> O. A. Kiselev,<sup>2</sup> J. V. Kratz,<sup>13</sup> R. Kulesa,<sup>14</sup> N. Kurz,<sup>2</sup> C. Langer,<sup>2,9</sup> M. Lantz,<sup>12,15</sup> T. Le Bleis,<sup>2,16</sup> R. Lemmon,<sup>17</sup> Yu. A. Litvinov,<sup>2</sup> K. Mahata,<sup>2,18</sup> C. Müntz,<sup>9</sup> T. Nilsson,<sup>12</sup> C. Nociforo,<sup>2</sup> G. Nyman,<sup>12</sup> W. Ott,<sup>2</sup> V. Panin,<sup>1,2</sup> S. Paschalis,<sup>2,7</sup> A. Perea,<sup>6</sup> R. Plag,<sup>2,9</sup> R. Reifarth,<sup>2,9</sup> A. Richter,<sup>1</sup> C. Rodríguez-Tajes,<sup>5</sup> D. Rossi,<sup>2,13,\*</sup> K. Riisager,<sup>11</sup> D. Savran,<sup>3,4</sup> G. Schrieder,<sup>1</sup> H. Simon,<sup>2</sup> J. Stroth,<sup>9</sup> K. Sümmerer,<sup>2</sup> O. Tengblad,<sup>6</sup> H. Weick,<sup>2</sup> C. Wimmer,<sup>2,9</sup> and M. V. Zhukov<sup>12</sup>

<sup>1</sup>*Institut für Kernphysik, Technische Universität Darmstadt, D-64289 Darmstadt, Germany*

<sup>2</sup>*GSI Helmholtzzentrum für Schwerionenforschung GmbH, D-64291 Darmstadt, Germany*

<sup>3</sup>*ExtreMe Matter Institute EMMI and Research Division GSI, D-64291 Darmstadt, Germany*

<sup>4</sup>*Frankfurt Institute for Advanced Studies FIAS, D-60438 Frankfurt am Main, Germany*

<sup>5</sup>*Departamento de Física de Partículas, Universidade de Santiago de Compostela, ES-15782 Santiago de Compostela, Spain*

<sup>6</sup>*Instituto de Estructura de la Materia, CSIC, ES-28006 Madrid, Spain*

<sup>7</sup>*Department of Physics, University of Liverpool, Liverpool L69 3BX, United Kingdom*

<sup>8</sup>*NRC Kurchatov Institute, RU-123182 Moscow, Russia*

<sup>9</sup>*Institut für Angewandte Physik, Goethe Universität, D-60438 Frankfurt am Main, Germany*

<sup>10</sup>*Department of Atomic, Molecular and Nuclear Physics, Universidad Complutense de Madrid, ES-28040 Madrid, Spain*

<sup>11</sup>*Department of Physics and Astronomy, University of Aarhus, DK-8000 Aarhus, Denmark*

<sup>12</sup>*Fundamental Fysik, Chalmers Tekniska Högskola, SE-41296 Göteborg, Sweden*

<sup>13</sup>*Institut für Kernchemie Johannes Gutenberg-Universität Mainz, D-55122 Mainz, Germany*

<sup>14</sup>*Instytut Fizyki, Uniwersytet Jagielloński, PL-30-059 Kraków, Poland*

<sup>15</sup>*Institutionen för fysik och astronomi, Uppsala Universitet, SE-75120 Uppsala, Sweden*

<sup>16</sup>*Physik-Department E12, Technische Universität München, D-85748 Garching, Germany*

<sup>17</sup>*Nuclear Physics Group, STFC Daresbury Lab, Warrington WA4 4AD, Cheshire, United Kingdom*

<sup>18</sup>*Nuclear Physics Division, Bhabha Atomic Research Centre, Trombay, Mumbai-400 085, India*

(Received 17 January 2014; published 4 April 2014)

We report on the first observation of the unbound proton-rich nucleus  $^{15}\text{Ne}$ . Its ground state and first excited state were populated in two-neutron knockout reactions from a beam of 500 MeV/u  $^{17}\text{Ne}$ . The  $^{15}\text{Ne}$  ground state is found to be unbound by 2.522(66) MeV. The decay proceeds directly to  $^{13}\text{O}$  with simultaneous two-proton emission. No evidence for sequential decay via the energetically allowed  $2^-$  and  $1^-$  states in  $^{14}\text{F}$  is observed. The  $^{15}\text{Ne}$  ground state is shown to have a strong configuration with two protons in the ( $sd$ ) shell around  $^{13}\text{O}$  with a 63(5)% ( $1s_{1/2}$ )<sup>2</sup> component.

DOI: 10.1103/PhysRevLett.112.132502

PACS numbers: 24.50.+g, 21.10.Dr, 25.60.-t, 27.20.+n

The availability of energetic beams of very short-lived exotic nuclei has largely increased the nuclear landscape in recent years by allowing experiments to produce and study a variety of different unbound nuclei and resonances, with distinct quantum properties. Experiments employing direct reactions in the neutron-rich region of the nuclear chart have reached resonances situated one or two neutron numbers beyond the neutron drip line, which is known up to the element oxygen ( $Z = 8$ ) [1]. The proton drip line, on the other hand, is known up to the element protactinium ( $Z = 91$ ) [2], and its position has been monitored by experiments on proton radioactivity [3]. The challenge for experiments and theory is to gather information needed for the understanding of the mechanism that destabilizes nuclei and to establish the limits of existence for resonances with measurable quantum signatures.

One- and two-neutron knockout reactions from radioactive beams of short-lived, already neutron-deficient nuclei provide effective methods for populating states of very exotic nuclear species beyond the proton drip line and for obtaining spectroscopic information about their dominant structures [4]. Similar to the two-proton knockout reactions, on the neutron-rich side of the nuclear chart [5], the two-neutron knockout from proton-rich nuclei is shown to be consistent with a direct knockout mechanism [6].

In this Letter we present the first observation of the unbound proton-rich nucleus  $^{15}\text{Ne}$  produced in two-neutron knockout reactions from a radioactive beam of  $^{17}\text{Ne}$ . Until now  $^{15}\text{Ne}$  is the lightest observed nucleus with isospin  $(T, T_z) = (5/2, -5/2)$ .

The radioactive beam was produced in fragmentation reactions in a Be target using a primary beam of  $^{20}\text{Ne}$  from

the heavy-ion synchrotron SIS at GSI. The secondary  $^{17}\text{Ne}$  beam, with an energy of 500 MeV/u, was identified on an event-by-event basis by energy loss, position, and TOF measurements. The beam was directed towards carbon or polyethylene reaction targets. The reaction products were identified by the magnetic rigidity from position measurements defining their trajectories in the magnetic field of a large-gap dipole magnet (ALADIN) placed behind the target. The protons and heavy fragments were guided into two separate arms, where additional energy loss and TOF measurements were performed. A schematic outline of the setup is given as Fig. 1 in Ref. [7]. The isotope identification plot for oxygen isotopes shown in Fig. 1 demonstrates that this setup selects  $^{13}\text{O}$  under very clean conditions, in spite of the much stronger intensities for the higher mass numbers. Coincidences between oxygen fragments and two protons provided momentum four vectors used in the analysis. The internal kinetic energy, that is, the relative energy  $E_{fpp}$  in the three-body  $^{15,14,13}\text{O} + p + p$  systems, as well as the fractional energies in the fragment-proton ( $\epsilon_{fp} = E_{fp}/E_{fpp}$ ) and the proton-proton ( $\epsilon_{pp} = E_{pp}/E_{fpp}$ ) subsystems, were determined.

The acceptance corrections and experimental  $E_{fpp}$  resolution were obtained from Monte Carlo simulations, comprising the ALADIN-R3B-setup response, and assuming isotropic three-body decays to  $^{15,14,13}\text{O} + 2p$  with different fixed  $E_{fpp}$  values between 0 and 10 MeV. The simulations showed that the response function for a resonance with zero width and  $E_{fpp} \geq 0.5$  MeV has a Gaussian shape, which is used for folding of the Breit-Wigner-shaped resonances. To benchmark the simulation, both concerning the energy dependence of the  $\sigma$  parameter in the Gaussian resolution function and the relative energy, we used the  $E_{fpp}$  spectrum for  $^{15}\text{O} + p + p$  shown in Fig. 2. One pronounced Gaussian-shaped peak is observed

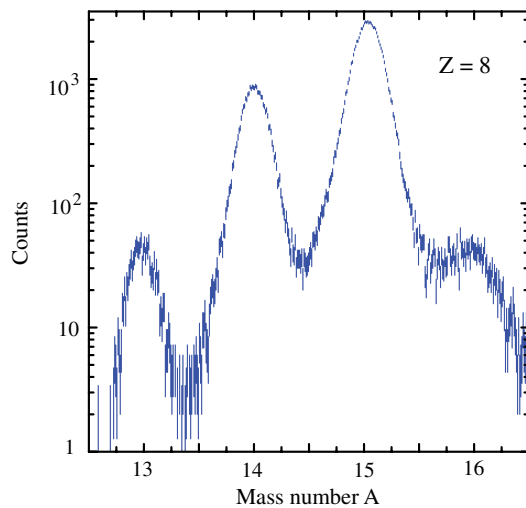


FIG. 1 (color online). Mass identification plot for final-state oxygen isotopes produced in the breakup of 500 MeV/u  $^{17}\text{Ne}$  projectiles on carbon and polyethylene targets.

at an energy of 881(5) keV. There are three low-lying states in  $^{17}\text{Ne}$  open to two-proton emission [8,9]. The first is a  $3/2^-$  state at  $E^* = 1.288$  MeV, which has been demonstrated to decay exclusively by  $\gamma$  emission and not by  $2p$  emission [9,10]. Further, there is a  $1/2^+$  state at  $E^* = 1.908$  MeV, which does not contribute to the spectrum in Fig. 2, since it is not strongly populated in inelastic scattering. The observed peak may therefore exclusively be assigned to the decay of the  $5/2^-$  state at  $E^* = 1.764(12)$  MeV, which has a negligible width compared to the experimental resolution [9,11]. The corresponding energy of the peak in the  $E_{fpp}$  spectrum is expected at 831(12) keV. The  $E_{fpp}$  energy calibration was adjusted accordingly. The observed width is entirely due to the experimental resolution and is therefore used as a benchmark for the parametrization of  $\sigma$  in the Gaussian resolution function, which is defined as  $\sigma = 0.183(4) \times E_{fpp}^{0.563}$ . The parameter in the exponent was determined from Monte Carlo simulations.

A further confirmation of the energy calibration and experimental resolution was obtained from an analysis of the  $^{14}\text{O} + p + p$  data. The relative-energy spectrum, which is shown in Fig. 3(a), features distinct resonances belonging to  $^{16}\text{Ne}$ . The resonance positions and, in some cases, the widths are known from earlier experiments KEK78, BUR80, WOO83, FOH97, MUK09. In the present analysis, the spectrum was decomposed into Breit-Wigner-shaped resonances folded with the experimental resolution in a least-squares fit. The fitting was performed using the function minimization and error analysis code MINUIT [12]. The relative intensities of the three pronounced resonances in Fig. 3(a) are 36.3(7)%, 6.5(6)%, and 14(2)%, respectively. The result of this analysis is given in Table I together with results from earlier experiments. Good agreement is found between the present and

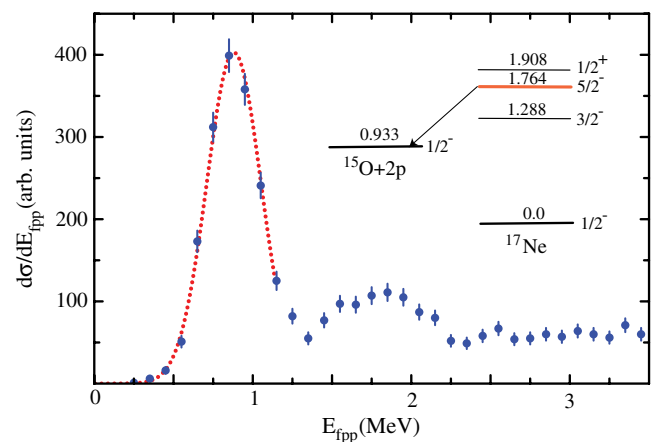


FIG. 2 (color online). The  $^{15}\text{O} + p + p$  relative-energy spectrum. The intense peak corresponding to the known  $^{17}\text{Ne}(5/2^-)$  state at an excitation energy of 1.764 MeV was used as benchmark for the experimental  $E_{fpp}$  resolution and for the fine-tuning of the energy calibration. The dotted line represents a Gaussian fit.

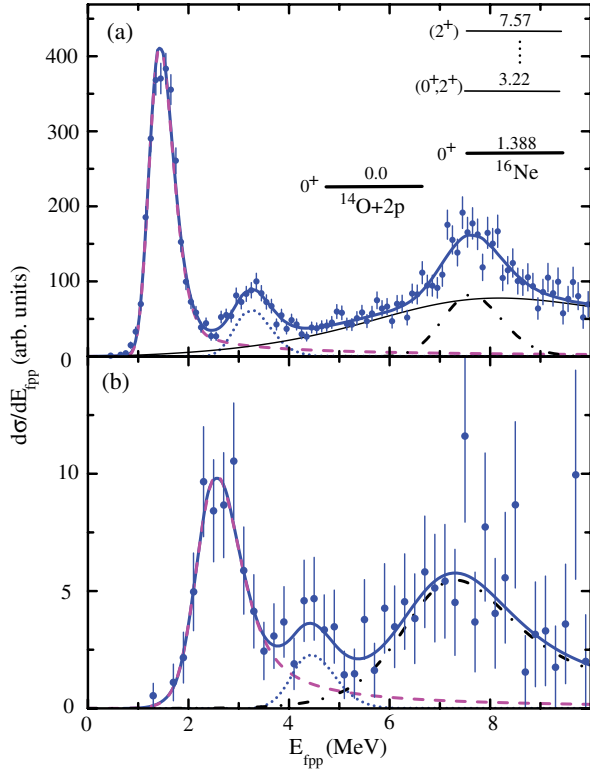


FIG. 3 (color online). (a) The  $^{14}\text{O} + p + p$  relative-energy spectrum used to verify the experimental resolution and the energy calibration (see Table I). The thin solid line extending below the spectrum is due to a nonresonant background. (b) The  $^{13}\text{O} + p + p$  relative-energy spectrum. The spectra are decomposed into several Breit-Wigner—shaped resonances convoluted with the experimental resolution.

published data for the positions of the three observed states and for the width of the ground-state resonance.

The analysis of the  $^{13}\text{O} + p + p$  relative energy spectrum was performed in the same manner as described above. The measured spectrum with the result of the fit is shown in Fig. 3(b). The ground state of  $^{15}\text{Ne}$  is identified at  $E_r = 2.522(66)$  MeV with  $\Gamma = 0.59(23)$  MeV. From mirror symmetry, this state is assigned to have spin-parity  $I^\pi = 3/2^-$ . The first excited state ( $I^\pi = 5/2^-$ ) was found at

TABLE I. Resonance energies ( $E_{fpp}$ ) and widths in MeV of  $^{16}\text{Ne}$  states as obtained in this experiment [ $\star$ ] together with results from earlier experiments.

$I^\pi = 0^+$		$I^\pi = (0^+, 2^+)$		$I^\pi = (2^+)$		Ref.
$E_r$	$\Gamma$	$E_r$	$\Gamma$	$E_r$	$\Gamma$	
1.388(15)	0.082(15)	3.22(5)	$\leq 0.05$	7.57(6)	$\leq 0.1$	[ $\star$ ]
1.33(8)	0.2(1)	3.02(11)	...	...	...	[13]
1.466(45)	...	...	...	...	...	[14]
1.399(24)	0.11(4)	...	...	...	...	[15]
...	...	3.5(2)	...	...	...	[16]
1.35(8)	...	...	...	7.6(2)	0.8( $\pm 8$ )	[17]

$E_r = 4.42(4)$  MeV with a narrow width,  $\Gamma \leq 0.1$  MeV. The relative intensities of the two observed resonances are 43.4(6)% and 7.3(3)%, respectively. The  $^{17}\text{Ne}$   $1n$  and  $2n$  knockout cross sections in the relative-energy interval  $0 < E_{fpp} < 10$  MeV for hydrogen and carbon were obtained as  $\sigma_{-1n}(\text{H}) = 15(3)$  mb and  $\sigma_{-1n}(\text{C}) = 20(4)$  mb and  $\sigma_{-2n}(\text{H}) = 1.2(6)$  mb and  $\sigma_{-2n}(\text{C}) = 1.3(6)$  mb. The 2.5 MeV broad distribution in the energy region 6—9 MeV most likely represents contributions from several unresolved resonances. The results are summarized in the level scheme shown in Fig. 4.

A major source of information about the decay mechanism of the  $^{15}\text{Ne}$  ground state may be obtained from the three-body energy correlations between the decay products in the final state. Two types of correlation functions were introduced. The first was defined as the distribution of fractional energy in the proton-proton subsystem  $W(\epsilon_{pp})$  and the second as the distribution of fractional energy in the fragment-proton subsystem  $W(\epsilon_{fp})$ . The fractional-energy distributions normalized to unity are shown in Figs. 5(a) and 5(b). The figure also includes the fractional-energy distributions derived from our data for  $^{16}\text{Ne}$  in the  $E_{fpp}$  region around its ground state.

The  $^{15}\text{Ne}$  ground state was found to be unstable towards  $^{13}\text{O} + p + p$  decay by 2.522(66) MeV, which corresponds to an atomic mass excess of  $\text{ME}(^{15}\text{Ne}) = 40.215(69)$  MeV. The mass excesses of the nuclei involved here were taken from Ref. [20]. Improved Garvey-Kelson mass relations, based on the mass differences of mirror nuclei, were recently proposed and masses of exotic proton-rich nuclei were determined [21,22]. The obtained mass-excess value,  $\text{ME}(^{15}\text{Ne}) = 41.555$  MeV with an uncertainty of  $\sigma = 23$  keV, deviates thus from the experimental value by about  $60\sigma$ . A simple argument to explain such deviations is given in Ref. [23] in terms of the pairing interaction. Recently, a value of  $\text{ME}(^{15}\text{Ne}) = 40.37(24)$  MeV, in good agreement with the present result, was estimated using a parametrization of the energy differences between known

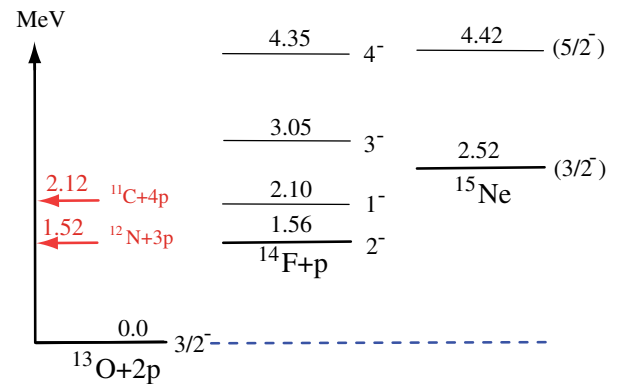


FIG. 4 (color online). Level schemes for  $^{15}\text{Ne}$  and daughter nuclei. The energies are given from zero internal energy in the  $^{13}\text{O} + p + p$  system. Thresholds for few-body decays are also shown. The energy levels for  $^{14}\text{F}$  are taken from Ref. [18].

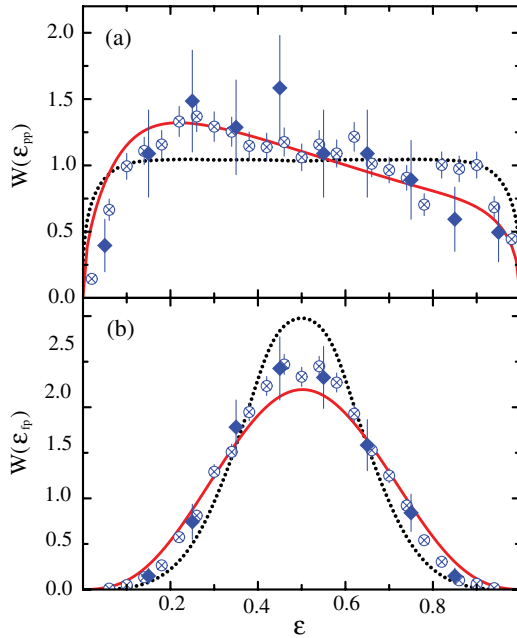


FIG. 5 (color online). Fractional energy spectra for  $^{15}\text{Ne}$  (diamond) and  $^{16}\text{Ne}$  (crossed circle). The distribution on fractional relative energy (a) between two protons and (b) between one proton and a  $^{13,14}\text{O}$  fragment for  $^{15,16}\text{Ne}$ , respectively, are shown as distributions normalized to unity. The solid lines are the results of theoretical calculations within a three-body model in the case of  $^{16}\text{Ne}$  [19]. The dotted lines show the result of a calculation assuming sequential decay of  $^{15}\text{Ne}$  via the ground state of  $^{14}\text{F}$ .

nuclei with  $N = 8, 10$  and their mirrors with  $Z = 8, 10$  [24]. In Ref. [24] it is shown that the ground states of  $N = 10$  nuclei may be reasonably well described as two neutrons in the ( $sd$ ) shell with spin zero coupled to a core predominantly in the  $p$  shell. The same structure is expected for mirror nuclei with  $Z = 10$  with two protons in the ( $sd$ ) shell, i.e.,  $^{13,14,15}\text{O} \otimes [\alpha(1s_{1/2})^2 + \beta(0d_{5/2})^2]$ . It was also shown that the difference between the two-nucleon binding energies ( $S_{2n}$  in  $N = 10$  and  $S_{2p}$  in  $Z = 10$ ) is directly related to the content of the  $s$  shell  $\alpha^2$ . The unknown binding energy of one of the mirror pairs can be estimated if  $\alpha^2$  and the binding energy of the other is known. Now, when the binding energies of  $^{15}\text{Ne}$  and  $^{15}\text{B}$  are both known, the content of  $s$ -shell protons can be estimated. The  $^{15}\text{Ne}$  ground state with spin-parity  $3/2^-$  may have a configuration mainly as  $^{13}\text{O} \otimes [\alpha(1s_{1/2})^2 + \beta(0d_{5/2})^2]$ , with the two valence protons coupled to spin zero. The estimated content of  $s$ -shell protons is then  $\alpha^2 = 63(5)\%$ , in agreement with Ref. [24].

The two-proton decay of a resonance state may be discussed in terms of three extreme scenarios: (i) a di-proton decay, (ii) a sequential decay through intermediate states in the  $fp$  subsystem, or (iii) as a genuine three-body decay with no strong interaction in any binary subsystem. The  $^{16}\text{Ne}$  ground state is bound relative to one-proton

emission while  $^{15}\text{Ne}$  has the possibility to decay with one-proton emission via the two lowest states in  $^{14}\text{F}$  (see Fig. 4), the  $2^-$  ground state at  $E_r = 1.56(4)$  MeV,  $\Gamma = 0.91(10)$  MeV and a  $1^-$  state at  $E_r = 2.10(17)$  MeV,  $\Gamma \approx 1$  MeV [18]. However, within statistical uncertainties in the fractional energy spectra, both nuclei exhibit the same pattern of correlations [see Figs. 5(a) and 5(b)]. There is thus no evidence for sequential decay of  $^{15}\text{Ne}$ .

The dotted lines in Fig. 5 correspond to sequential proton emission through the ground state of  $^{14}\text{F}$  in  $R$  matrix formalism, described in Ref. [25]. The results are clearly not in accordance with the experimentally observed correlations. The solid lines demonstrate the result of a calculation within a three-body model for  $^{16}\text{Ne}$  [19]. The calculations are in good agreement with the experimental  $W(\epsilon_{pp})$  and  $W(\epsilon_{fp})$  distributions and demonstrate that no characteristic features of the sequential emission from  $^{15}\text{Ne}$  through  $^{14}\text{F}$  states were observed. The distributions are wide and the decay mechanism is of neither di-proton nor sequential type. The conclusion is, therefore, that we are faced with a genuine three-body, i.e., democratic, decay. The Coulomb focusing effect can clearly be observed in the  $W(\epsilon_{fp})$  distribution. Because of the strong Coulomb repulsion from the fragment, the protons are forming a more narrow distribution, centered at  $\epsilon_{fp} = 0.5$ . Note that the relative energy between protons  $E_{pp}$  at the same time may be as large as the total internal energy in the three-body system. The enhancement seen in the  $W(\epsilon_{pp})$  distribution at low  $\epsilon_{pp}$  reveals features of the proton-proton interaction in the final state.

The first excited state in  $^{15}\text{Ne}$  was identified at 4.42(4) MeV above the  $^{13}\text{O} + p + p$  threshold, i.e., at an excitation energy  $E^* = 1.90(8)$  MeV. This energy may be compared with the position of the  $I^\pi = 5/2^-$  state in the mirror nucleus  $^{15}\text{B}$  at  $E^* = 1.327(12)$  MeV [26]. The 0.57(8) MeV energy difference, the Thomas-Ehrman shift, originates in the broad radial distribution of the proton single-particle wave function [27].

Furthermore, the ground state of  $^{15}\text{Ne}$  is unstable towards three-proton emission by 1.0 MeV and to four-proton emission by 0.4 MeV (see Fig. 4). As a future perspective, studies of these decay channels could provide additional information about the structure of the neon isotopes at the edge of existence.

In summary, we have observed for the first time the unbound nucleus  $^{15}\text{Ne}$ , which until now is the lightest observed  $T_z = -5/2$  nucleus. Using one- and two-neutron knockout reactions from a radioactive beam of  $^{17}\text{Ne}$ , benchmarking on  $^{17}\text{Ne}$  as a calibration, the energies and widths of states in  $^{15}\text{Ne}$  as well as in  $^{16}\text{Ne}$  were obtained. An atomic-mass excess of 40.215(69) MeV for the  $^{15}\text{Ne}$  ground state was determined, which means a 2.522(66) MeV instability with respect to  $^{13}\text{O} + p + p$  decay. The energy correlations between the decay products of the  $^{15}\text{Ne}$  ground state indicate a democratic decay

mechanism. The value of the position of the  $^{15}\text{Ne}$  ground state was used to determine its main structure as  $^{13}\text{O} \otimes [\alpha(1s_{1/2})^2 + \beta(0d_{5/2})^2]$  with a 63(5)% of  $(1s_{1/2})^2$  component.

The authors are indebted to I. A. Egorova and L. V. Grigorenko for fruitful discussions. The authors acknowledge support from Russian Foundation for Basic Research (RFBR Grant No. 12-02-01115-a), the Spanish research agency CICYT under Project No. FPA2009-07387, the Helmholtz Alliance EMMI, HIC for FAIR, the GSI-TU Darmstadt cooperation agreement, and the BMBF under Contract No. 05P12RDFN8. B.J. is a Helmholtz International Fellow.

---

\*Present address: National Superconducting Cyclotron Laboratory, MSU, East Lansing, MI 48824, USA.

- [1] H. Simon, *Phys. Scr.* **T152**, 014024 (2013).
- [2] M. Thoennessen, *Rep. Prog. Phys.* **67**, 1187 (2004).
- [3] M. Pfützner, *Phys. Scr.* **T152**, 014014 (2013).
- [4] P. G. Hansen and J. A. Tostevin, *Annu. Rev. Nucl. Part. Sci.* **53**, 219 (2003).
- [5] D. Bazin *et al.*, *Nucl. Phys.* **A746**, 173 (2004).
- [6] K. Yoneda *et al.*, *Phys. Rev. C* **74**, 021303(R) (2006).
- [7] C. Langer *et al.*, *Phys. Rev. C* **89**, 035806 (2014).
- [8] V. Guimarães *et al.*, *Phys. Rev. C* **58**, 116 (1998).
- [9] M. J. Chromik *et al.*, *Phys. Rev. C* **66**, 024313 (2002).
- [10] T. Zerguerras *et al.*, *Eur. Phys. J. A* **20**, 389 (2004).
- [11] E. Garrido, D. V. Fedorov, A. S. Jensen, H. O. U. Fynbo, *Nucl. Phys.* **A748**, 39 (2005).
- [12] F. James and M. Roos, *Comput. Phys. Commun.* **10**, 343 (1975).
- [13] G. KeKelis, M. Zisman, D. Scott, R. Jahn, D. Vieira, Joseph Cerny, and F. Ajzenberg-Selove, *Phys. Rev. C* **17**, 1929 (1978).
- [14] G. R. Bureson *et al.*, *Phys. Rev. C* **22**, 1180 (1980).
- [15] C. J. Woodward, R. E. Tribble, and D. M. Tanner, *Phys. Rev. C* **27**, 27 (1983).
- [16] K. Föhl *et al.*, *Phys. Rev. Lett.* **79**, 3849 (1997).
- [17] I. Mukha *et al.*, *Phys. Rev. C* **79**, 061301(R) (2009).
- [18] V. Z. Goldberg *et al.*, *Phys. Lett. B* **692**, 307 (2010).
- [19] L. V. Grigorenko, I. G. Mukha, I. J. Thompson, and M. V. Zhukov, *Phys. Rev. Lett.* **88**, 042502 (2002).
- [20] M. Wang, G. Audi, A. H. Wapstra, F. G. Kondev, M. MacCormick, X. Xu, and B. Pfeiffer, *Chin. Phys. C* **36**, 1603 (2012).
- [21] J. Tian, N. Wang, C. Li, and J. Li, *Phys. Rev. C* **87**, 014313 (2013).
- [22] M. Bao, Z. He, Y. Lu, Y. M. Zhao, and A. Arima, *Phys. Rev. C* **88**, 064325 (2013).
- [23] Z. He, M. Bao, Y. M. Zhao, and A. Arima, *Phys. Rev. C* **87**, 057304 (2013).
- [24] H. T. Fortune, *Phys. Lett. B* **718**, 1342 (2013).
- [25] F. C. Barker, *Phys. Rev. C* **59**, 535 (1999).
- [26] M. Stanoiu *et al.*, *Eur. Phys. J. A* **22**, 5 (2004).
- [27] K. Ogawa, H. Nakada, S. Hino, and R. Motegi, *Phys. Lett. B* **464**, 157 (1999).